

PHYSICO-CHEMICAL PROCESSES IN ICE AND PERMAFROST
ION-INDUCED NUCLEATION: A NEW THEORETICAL MODEL

V.A. Vlasov, G.V. Anikin

*Institute of the Earth Cryosphere, Siberian Branch of the Russian Academy of Sciences,
P/O box 1230, Tyumen, 625000, Russia; vlasov.ikz@gmail.com, anikin@ikz.ru*

The paper presents a new theoretical model of nucleation on ions located randomly relative to the forming phase, including outside the clusters of the new phase. In the case of ions inside the new phase, the energy of their interaction with the surrounding molecules expressed via the parameter q can be taken into account explicitly. The best fit of the theoretical predictions to experimental data on condensation of supersaturated vapor can be found by varying q for different materials, which shows temperature dependence.

Heterogeneous nucleation, ions, nucleation work, nucleation rate

INTRODUCTION

Physics of permafrost-related processes deals a lot with issues of condensation, desublimation, and crystallization of water, including the stage of nucleation [Anisimov, 2003]. Nucleation occurs in the atmosphere due to the presence of ions produced by cosmic radiation, and is relevant to formation of clouds or snow [Matveev, 1965].

Many theoretical studies consider ion-induced nucleation in terms of the classical thermodynamic approach [Thomson and Thomson, 1933; Tohmfor and Volmer, 1938; Russell, 1969; Kortzeborn and Abraham, 1973; Rusanov, 1979; Rusanov and Kuni, 1984; Vorobiev and Malysenko, 2001; Toshev, 2002; Nadykto and Yu, 2004; Fisenko et al., 2005], proceeding from Thomson's model with ions inside the clusters of the forming phase. However, there are first-kind phase transitions implying the existence of ions outside these clusters, such as ions of impurities expelled by ice that forms on water crystallization [Hobbs, 1974]. According to simulation results, ions can be also pushed out to the periphery of ionic clusters during condensation of water vapor on chlorine ions [Shevkunov, 2002a,b; Dang and Smith, 1993]. Furthermore, the theoretical studies based on Thomson's model neglect the energy of interaction between the ions and the molecules of the new phase in the clusters [Kusaka et al., 1995a,b; Brodskaya et al., 2002; Nadykto et al., 2006].

Thus, there is a need in a new model which would be free from all these drawbacks and be universal, i.e., applicable to any first-kind phase transition. Such a model is suggested in this paper.

THEORY

Nucleation work. The work required to form a spherical cluster of a new phase within an existing (old) phase can be written as [Anikin, 2004; Anikin and Plotnikov, 2005]

$$W_{\text{out}} = E_s \left(-\frac{2}{3}y^3 + y^2 - \frac{p}{y} \sum_{l=0}^{\infty} \frac{\epsilon_{\text{new}}^l}{\epsilon_{\text{new}}^l + \epsilon_{\text{old}}(l+1)} \left(\frac{y}{z} \right)^{2(l+1)} \right),$$

$$z > y + u, y > 0, \quad (1)$$

for an ion located outside the cluster (Fig. 1, a), or as

$$W_{\text{in}} = E_s \left(-\frac{2}{3}y^3 + y^2 + \frac{p}{y} \sum_{l=0}^{\infty} \frac{\epsilon_{\text{old}}(l+1)}{\epsilon_{\text{new}}^l + \epsilon_{\text{old}}(l+1)} \left(\frac{z}{y} \right)^{2l} + q_0 \right),$$

$$z < y - u, y > u, \quad (2)$$

for an ion fully inside the cluster (Fig. 1, b). There ϵ_{old} and ϵ_{new} are the static dielectric permittivities of the old and new phases, respectively; q_0 is the dimensionless parameter that refers to the interaction of the ion with the surrounding molecules of the cluster and accounts for the ion size and the type of phase transition;

$$E_s = 4\pi\sigma R_0^2, \quad p = \frac{(eZ)^2 (\epsilon_{\text{new}} - \epsilon_{\text{old}})}{32\pi^2 \epsilon_0 \epsilon_{\text{new}} \epsilon_{\text{old}} \sigma R_0^3},$$

$$y = \frac{R}{R_0}, \quad z = \frac{r}{R_0}, \quad u = \frac{R_{\text{ion}}}{R_0},$$

where e is the elementary electrical charge; Z is the ion charge ratio; ϵ_0 is the electric constant; σ is the surface tension between the old and new phases; R_0 is the critical radius of homogeneous nucleation

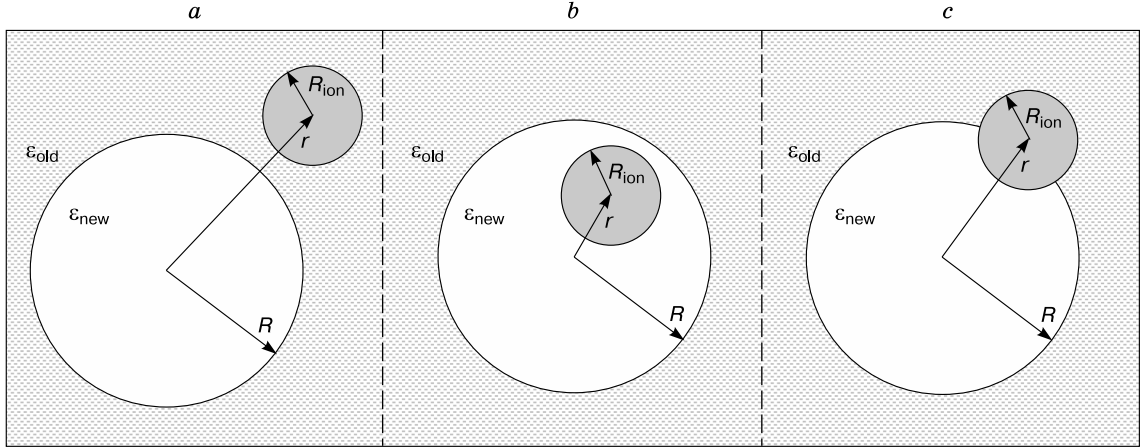


Fig. 1. Formation of a spherical cluster of a new phase within an old phase, with an ion outside (a) or inside (b) the cluster, or at the new-old phase interface (c).

($p = q_0 = u = 0$); R is the radius of the forming cluster; R_{ion} is the ion radius; r is the distance between the ion and the cluster center (Fig. 1). The parameter E_s refers to the surface energy of a critical cluster in the case of homogeneous nucleation.

Equations (1) and (2) become

$$W_{\text{out}} = E_s f_{\text{out}}(y, z), \quad z > y + u, \quad y > 0; \quad (3)$$

$$W_{\text{in}} = E_s f_{\text{in}}(y, z), \quad z < y - u, \quad y > u, \quad (4)$$

where

$$f_{\text{out}}(y, z) = -\frac{2}{3}y^3 + y^2 - \frac{p}{y} \sum_{l=0}^{\infty} \frac{\epsilon_{\text{new}}^l}{\epsilon_{\text{new}}^l + \epsilon_{\text{old}}(l+1)} \left(\frac{y}{z}\right)^{2(l+1)}; \quad (5)$$

$$f_{\text{in}}(y, z) = -\frac{2}{3}y^3 + y^2 + \frac{p}{y} \sum_{l=0}^{\infty} \frac{\epsilon_{\text{old}}(l+1)}{\epsilon_{\text{new}}^l + \epsilon_{\text{old}}(l+1)} \left(\frac{z}{y}\right)^{2l} + q_0. \quad (6)$$

In the case when the ion is located at the interface of the spherical cluster with the old phase (Fig. 1, c), the nucleation work will be

$$W_{\text{inter}} = E_s f_{\text{inter}}(y, z), \quad y - u \leq z \leq y + u, \quad y > u, \quad (7)$$

where the function $f_{\text{inter}}(y, z)$ is approximated by the third-degree polynomial:

$$f_{\text{inter}}(y, z) = a(z) + b(z)y + c(z)y^2 + d(z)y^3.$$

The unknowns in this equation are found from the continuity condition for the nucleation work function and its first derivative along y at $y = z + u$ and $y = z - u$:

$$f_{\text{in}}(y, z)|_{y=z+u} = f_{\text{inter}}(y, z)|_{y=z+u},$$

$$f_{\text{inter}}(y, z)|_{y=z-u} = f_{\text{out}}(y, z)|_{y=z-u},$$

$$\frac{\partial f_{\text{in}}(y, z)}{\partial y} \Big|_{y=z+u} = \frac{\partial f_{\text{inter}}(y, z)}{\partial y} \Big|_{y=z+u}, \quad (8)$$

$$\frac{\partial f_{\text{inter}}(y, z)}{\partial y} \Big|_{y=z-u} = \frac{\partial f_{\text{out}}(y, z)}{\partial y} \Big|_{y=z-u}.$$

Solving the systems of equations (8) with respect to the unknowns gives

$$d(z) = \frac{1}{4u^2} \left(\frac{\partial f_{\text{in}}(y, z)}{\partial y} \Big|_{y=z+u} + \frac{\partial f_{\text{out}}(y, z)}{\partial y} \Big|_{y=z-u} + \frac{1}{u} f_{\text{out}}(y, z) \Big|_{y=z-u} - \frac{1}{u} f_{\text{in}}(y, z) \Big|_{y=z+u} \right),$$

$$c(z) = \frac{1}{4u} \left(\frac{\partial f_{\text{in}}(y, z)}{\partial y} \Big|_{y=z+u} - \frac{\partial f_{\text{out}}(y, z)}{\partial y} \Big|_{y=z-u} \right) - 3zd(z), \quad (9)$$

$$b(z) = \frac{\partial f_{\text{out}}(y, z)}{\partial y} \Big|_{y=z-u} - 2(z-u)c(z) - 3(z-u)^2 d(z),$$

$$a(z) = f_{\text{out}}(y, z) \Big|_{y=z-u} - (z-u)b(z) -$$

$$-(z-u)^2 c(z) - (z-u)^3 d(z).$$

Taking into account (5) and (6), it is easy to obtain explicit expressions for (9).

Function extremes. The model of ion-induced nucleation includes the extremes of the functions W_{in} , W_{out} and W_{inter} (see below) found as local extremes of the functions $f_{\text{in}}(y, z)$, $f_{\text{out}}(y, z)$ and $f_{\text{inter}}(y, z)$ taking into account (3), (4) and (7). Hereafter it is assumed that $p > 0$ ($\epsilon_{\text{new}} > \epsilon_{\text{old}}$).

With the introduced parameter $\theta = (z/y)^2$, the function $f_{in}(y, z)$ can reach its local extremes along the parametrically specified lines

$$y_{in1}(\theta) = \frac{1}{4} + \frac{1}{2}\sqrt{\frac{1}{4} + x(\theta)} + \sqrt{\left(\frac{1}{4} + \frac{1}{2}\sqrt{\frac{1}{4} + x(\theta)}\right)^2 - \frac{x(\theta)}{2} - \sqrt{\frac{x^2(\theta)}{4} - \frac{pF_1(\theta)}{2}}},$$

$$z_{in1}(\theta) = y_{in1}(\theta)\sqrt{\theta}, \quad 0 \leq \theta \leq \theta_{in2}; \quad (10)$$

$$y_{in2}(\theta) = \frac{1}{4} + \frac{1}{2}\sqrt{\frac{1}{4} + x(\theta)} - \sqrt{\left(\frac{1}{4} + \frac{1}{2}\sqrt{\frac{1}{4} + x(\theta)}\right)^2 - \frac{x(\theta)}{2} - \sqrt{\frac{x^2(\theta)}{4} - \frac{pF_1(\theta)}{2}}},$$

$$z_{in2}(\theta) = y_{in2}(\theta)\sqrt{\theta}, \quad 0 \leq \theta \leq \theta_{in2}, \quad (11)$$

where

$$x(\theta) = \sqrt[3]{\frac{pF_1(\theta)}{4} + \sqrt{\frac{p^2F_1^2(\theta)}{16} - \frac{8p^3F_1^3(\theta)}{27}}} + \sqrt[3]{\frac{pF_1(\theta)}{4} - \sqrt{\frac{p^2F_1^2(\theta)}{16} - \frac{8p^3F_1^3(\theta)}{27}}},$$

$$F_1(\theta) = \sum_{l=0}^{\infty} \frac{\varepsilon_{old}(l+1)(2l+1)\theta^l}{\varepsilon_{new}l + \varepsilon_{old}(l+1)}.$$

Line (10) corresponds to local maximums at $0 \leq \theta \leq \theta_{in1}$ and to local minimums at $\theta_{in1} \leq \theta \leq \theta_{in2}$, while (11) is a line of local minimums; θ_{in1} and θ_{in2} are the roots of transcendent equations of the form

$$y_{in1}^3(\theta_{in1}) - 2y_{in1}^4(\theta_{in1}) + pF_2(\theta_{in1}) = 0, \quad (12)$$

$$pF_1(\theta_{in2}) = p_{cr} = 0,210\,937\,5,$$

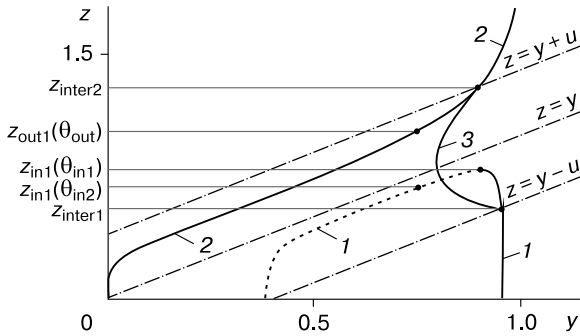


Fig. 2. Local extremes of the functions $f_{in}(y, z)$ (curve 1), $f_{out}(y, z)$ (curve 2) and $f_{inter}(y, z)$ (curve 3).

Solid and dash lines, respectively, correspond to local maximums and minimums; $p = 0.07$, $\varepsilon_{new}/\varepsilon_{old} = 40$, $q_0 = -0.27$, $u = 0.4$.

where

$$F_2(\theta) = \sum_{l=0}^{\infty} \frac{\varepsilon_{old}(l+1)^2(2l+1)\theta^l}{\varepsilon_{new}l + \varepsilon_{old}(l+1)},$$

and p_{cr} is the critical parameter: barrierless nucleation can take place at $p_{cr} \leq pF_1(\theta)$. Solving (12) gives θ_{in1} and θ_{in2} .

Judging by the positions of its local extremes, the function $f_{out}(y, z)$ has only lines of local maximums specified parametrically as

$$y_{out1}(\theta) = \frac{1}{4} + \frac{1}{2}\sqrt{\frac{1}{4} + g(\theta)} + \sqrt{\left(\frac{1}{4} + \frac{1}{2}\sqrt{\frac{1}{4} + g(\theta)}\right)^2 - \frac{g(\theta)}{2} - \sqrt{\frac{g^2(\theta)}{4} - \frac{pQ(\theta)}{2}}},$$

$$z_{out1}(\theta) = y_{out1}(\theta)\sqrt{\theta}, \quad \theta_{out} \leq \theta; \quad (13)$$

$$y_{out2}(\theta) = \frac{1}{4} + \frac{1}{2}\sqrt{\frac{1}{4} + g(\theta)} - \sqrt{\left(\frac{1}{4} + \frac{1}{2}\sqrt{\frac{1}{4} + g(\theta)}\right)^2 - \frac{g(\theta)}{2} - \sqrt{\frac{g^2(\theta)}{4} - \frac{pQ(\theta)}{2}}},$$

$$z_{out2}(\theta) = y_{out2}(\theta)\sqrt{\theta}, \quad \theta_{out} \leq \theta, \quad (14)$$

where

$$g(\theta) = \sqrt[3]{\frac{pQ(\theta)}{4} + \sqrt{\frac{p^2Q^2(\theta)}{16} - \frac{8p^3Q^3(\theta)}{27}}} + \sqrt[3]{\frac{pQ(\theta)}{4} - \sqrt{\frac{p^2Q^2(\theta)}{16} - \frac{8p^3Q^3(\theta)}{27}}},$$

$$Q(\theta) = \sum_{l=0}^{\infty} \frac{\varepsilon_{new}(2l+1)\theta^{-(l+1)}}{\varepsilon_{new}l + \varepsilon_{old}(l+1)}.$$

Lines (13) and (14) are the branches of a single curve that meet at $\theta = \theta_{out}$, while θ_{out} is found by solving the transcendent equation

$$pQ(\theta_{out}) = p_{cr} = 0,210\,937\,5.$$

As we can show, the function $f_{inter}(y, z)$ has only a line of local maximums in its domain of definition ($y-u \leq z \leq y+u$, $y > u$), and this line is given by

$$y_{inter}(z) = -\frac{1}{3} \left(\frac{c(z) + \sqrt{c^2(z) - 3d(z)b(z)}}{d(z)} \right),$$

$$y_{inter}(z) - u \leq z \leq y_{inter}(z) + u. \quad (15)$$

The curves of local extremes calculated with (10), (11), (13)–(15) for a specific case are shown in Fig. 2.

Then the values of the respective functions $f_{\text{in}}(y, z)$, $f_{\text{out}}(y, z)$ and $f_{\text{inter}}(y, z)$ can be found proceeding from the known position of the local maximum line. Namely,

$$f_{\text{in}}^{\text{max}} = f_{\text{in}}^{\text{max}}(\theta) = -\frac{2}{3}y_{\text{in}1}^3(\theta) + y_{\text{in}1}^2(\theta) + \frac{p}{y_{\text{in}1}(\theta)} \sum_{l=0}^{\infty} \frac{\varepsilon_{\text{old}}(l+1)\theta^l}{\varepsilon_{\text{new}}l + \varepsilon_{\text{old}}(l+1)} + q_0,$$

$$0 \leq \theta \leq \theta_{\text{in}1};$$

$$f_{\text{out}}^{\text{max}1} = f_{\text{out}}^{\text{max}1}(\theta) = -\frac{2}{3}y_{\text{out}1}^3(\theta) + y_{\text{out}1}^2(\theta) - \frac{p}{y_{\text{out}1}(\theta)} \sum_{l=0}^{\infty} \frac{\varepsilon_{\text{new}}l\theta^{-(l+1)}}{\varepsilon_{\text{new}}l + \varepsilon_{\text{old}}(l+1)},$$

$$\theta_{\text{out}} \leq \theta;$$

$$f_{\text{out}}^{\text{max}2} = f_{\text{out}}^{\text{max}2}(\theta) = -\frac{2}{3}y_{\text{out}2}^3(\theta) + y_{\text{out}2}^2(\theta) - \frac{p}{y_{\text{out}2}(\theta)} \sum_{l=0}^{\infty} \frac{\varepsilon_{\text{new}}l\theta^{-(l+1)}}{\varepsilon_{\text{new}}l + \varepsilon_{\text{old}}(l+1)},$$

$$\theta_{\text{out}} \leq \theta;$$

$$f_{\text{inter}}^{\text{max}} = f_{\text{inter}}^{\text{max}}(z) = a(z) + b(z)y_{\text{inter}}(z) + c(z)y_{\text{inter}}^2(z) + d(z)y_{\text{inter}}^3(z),$$

$$y_{\text{inter}}(z) - u \leq z \leq y_{\text{inter}}(z) + u.$$

The values of the function $f_{\text{in}}(y, z)$ along the local minimum line are found in a similar way.

Nucleation rate. The rate at which a phase nucleates within an old phase in the presence of ions can be written as [Anikin and Plotnikov, 2007]

$$J = N_1 n \nu R_0^2 j \int_0^{z_{\text{max}}} \left(\int_{\delta}^{\infty} \exp\left[\frac{W(y, z)}{kT}\right] dy \right)^{-1} 4\pi z^2 dz, \quad (16)$$

where N_1 is the concentration of isolated molecules in the old phase; n is the concentration of ions; ν is the volume of a single molecule in the new phase; j is the flux of molecules adjoining the cluster, which depends on the external thermodynamic conditions, on the origin of material subject to the phase change, and on the type of this change; $W(y, z)$ is the nucleation work, which is described by (3), (4), or (7) depending on the function definition domain and is in the general form $W(y, z) = E_s f(y, z)$; k is the Boltzmann constant; T is the temperature;

$$z_{\text{max}} = \frac{1}{R_0} \sqrt[3]{\frac{3}{4\pi n}}, \quad \delta = \frac{1}{R_0} \sqrt[3]{\frac{3\nu}{4\pi}}.$$

The nucleation rate written as (16) applies to any phase transition, and (16) is its most universal expression in this sense.

The J/J_0 ratio of nucleation rates, where J and J_0 correspond to nucleation on ions and homogeneous or spontaneous nucleation, respectively, is found with J_0 being generally [Strickland-Constable, 1968]:

$$J_0 = 2N_1 j \nu \sqrt{\frac{\sigma}{kT}} \exp\left[-\frac{E_s}{3kT}\right], \quad (17)$$

and for a spherical cluster,

$$J_0 = \frac{N_1 j \nu}{R_0} \sqrt{\frac{E_s}{\pi kT}} \exp\left[-\frac{E_s}{3kT}\right]. \quad (18)$$

With regard to (18), equation (16) becomes

$$J = N_1 n \nu R_0^2 j \int_0^{z_{\text{max}}} \left(\int_{\delta}^{\infty} \exp\left[\frac{E_s f(y, z)}{kT}\right] dy \right)^{-1} 4\pi z^2 dz + J_0 - J_0 =$$

$$= J_0 + N_1 n \nu R_0^2 j \sqrt{\frac{E_s}{\pi kT}} \left(\sqrt{\frac{\pi kT}{E_s}} \int_0^{z_{\text{max}}} \left(\int_{\delta}^{\infty} \exp\left[\frac{E_s f(y, z)}{kT}\right] dy \right)^{-1} \times \right.$$

$$\left. \times 4\pi z^2 dz - \frac{4\pi z_{\text{max}}^3}{3} \exp\left[-\frac{E_s}{3kT}\right] \right).$$

Dividing it by (18) gives the sought ratio:

$$\frac{J}{J_0} = 1 + n R_0^3 \exp\left[\frac{E_s}{3kT}\right] \left(\sqrt{\frac{\pi kT}{E_s}} \int_0^{z_{\text{max}}} \left(\int_{\delta}^{\infty} \exp\left[\frac{E_s f(y, z)}{kT}\right] dy \right)^{-1} \times \right.$$

$$\left. \times 4\pi z^2 dz - \frac{4\pi z_{\text{max}}^3}{3} \exp\left[-\frac{E_s}{3kT}\right] \right). \quad (19)$$

Equation (19) for the J/J_0 ratio is of special importance as it allows comparing quantitatively the nucleation rates in the presence of ions and in their absence (spontaneous nucleation), i.e., (19) shows explicitly how ions can influence the nucleation rate.

Like (16), equation (19) is a key one in the suggested model. The double integral in it can be found only numerically, but then it becomes possible to apply numerical integration of single-variable functions using the method of steepest descent (saddle point):

$$\int_{\delta}^{\infty} \exp\left[\frac{E_s f(y, z)}{kT}\right] dy \approx$$

$$\approx \sqrt{\frac{2\pi kT}{E_s}} \exp\left[\frac{E_s f_{\text{max}}}{kT}\right] \left(\sqrt{\left| \frac{\partial^2 f(y_{\text{max}}, z)}{\partial y^2} \right|} \right)^{-1}. \quad (20)$$

This approximation is valid at $E_s f_{\text{max}}/(kT) \gg 1$. Substituting (20) into (19) and taking into account the definition domains of the functions $f_{\text{in}}(y, z)$,

$f_{\text{out}}(y, z)$ and $f_{\text{inter}}(y, z)$, for the case of $p > 0$, we obtain

$$\begin{aligned} \frac{J}{J_0} = & 1 + nR_0^3 \exp\left[\frac{E_s}{3kT}\right] \times \\ & \times \left(\int_0^{z_{\text{inter1}}} \sqrt{\frac{1}{2} \left| \frac{\partial^2 f_{\text{in}}(y_{\text{max}}, z)}{\partial y^2} \right|} \exp\left[-\frac{E_s f_{\text{in}}^{\text{max}}}{kT}\right] 4\pi z^2 dz + \right. \\ & + \int_{z_{\text{inter1}}}^{z_{\text{inter2}}} \sqrt{\frac{1}{2} \left| \frac{\partial^2 f_{\text{inter}}(y_{\text{max}}, z)}{\partial y^2} \right|} \exp\left[-\frac{E_s f_{\text{inter}}^{\text{max}}}{kT}\right] 4\pi z^2 dz + \\ & + \left. \int_{z_{\text{inter2}}}^{z_{\text{max}}} \sqrt{\frac{1}{2} \left| \frac{\partial^2 f_{\text{out}}(y_{\text{max}}, z)}{\partial y^2} \right|} \exp\left[-\frac{E_s f_{\text{out}}^{\text{max1}}}{kT}\right] 4\pi z^2 dz - \right. \\ & \left. - \frac{4\pi z_{\text{max}}^3}{3} \exp\left[-\frac{E_s}{3kT}\right] \right), \end{aligned}$$

where z_{inter1} is the z coordinate of the point where the curve of local maximums of the function $f_{\text{in}}(y, z)$ crosses $z = y - u$; z_{inter2} is the z coordinate of the point where the curve of local maximums of $f_{\text{out}}(y, z)$ crosses $z = y + u$ (Fig. 2). In the first and third integrals, we proceed from integration along z to that along θ , bearing in mind that it follows the line of local maximums:

$$\begin{aligned} \frac{J}{J_0} = & 1 + nR_0^3 \exp\left[\frac{E_s}{3kT}\right] \times \\ & \times \left(\int_0^{\theta_{\text{inter1}}} 4\pi \sqrt{|f_{\text{in}}''(\theta)|} \exp\left[-\frac{E_s f_{\text{in}}^{\text{max}}(\theta)}{kT}\right] y_{\text{in1}}^2(\theta) \theta \left(\frac{dz}{d\theta}\right)_{\text{in}}^{\text{max}} d\theta + \right. \\ & + \int_{z_{\text{inter1}}}^{z_{\text{inter2}}} 4\pi \sqrt{|f_{\text{inter}}''(z)|} \exp\left[-\frac{E_s f_{\text{inter}}^{\text{max}}(z)}{kT}\right] z^2 dz + \\ & + \int_{\theta_{\text{inter2}}}^{\theta_{\text{max}}} 4\pi \sqrt{|f_{\text{out}}''(\theta)|} \exp\left[-\frac{E_s f_{\text{out}}^{\text{max1}}(\theta)}{kT}\right] \times \\ & \times y_{\text{out1}}^2(\theta) \theta \left(\frac{dz}{d\theta}\right)_{\text{out}}^{\text{max}} d\theta - \frac{4\pi z_{\text{max}}^3}{3} \exp\left[-\frac{E_s}{3kT}\right] \left. \right), \quad (21) \end{aligned}$$

where

$$\begin{aligned} f_{\text{in}}''(\theta) &= \frac{1}{2} \frac{\partial^2 f_{\text{in}}(y_{\text{max}}, z)}{\partial y^2} \\ &= 1 - 2y_{\text{in1}}(\theta) + \frac{p}{y_{\text{in1}}^3(\theta)} \sum_{l=0}^{\infty} \frac{\varepsilon_{\text{old}}(l+1)^2 (2l+1) \theta^l}{\varepsilon_{\text{new}} l + \varepsilon_{\text{old}}(l+1)}, \\ f_{\text{inter}}''(z) &= \frac{1}{2} \frac{\partial^2 f_{\text{inter}}(y_{\text{max}}, z)}{\partial y^2} = c(z) + 3d(z) y_{\text{inter}}(z), \\ f_{\text{out}}''(\theta) &= \frac{1}{2} \frac{\partial^2 f_{\text{out}}(y_{\text{max}}, z)}{\partial y^2} \\ &= 1 - 2y_{\text{out1}}(\theta) - \frac{p}{y_{\text{out1}}^3(\theta)} \sum_{l=0}^{\infty} \frac{\varepsilon_{\text{new}} l^2 (2l+1) \theta^{-(l+1)}}{\varepsilon_{\text{new}} l + \varepsilon_{\text{old}}(l+1)}, \end{aligned}$$

$$\begin{aligned} \left(\frac{dz}{d\theta}\right)_{\text{in}}^{\text{max}} &= \\ &= \left[4y_{\text{in1}}^4(\theta) - 3y_{\text{in1}}^3(\theta) - p \sum_{l=0}^{\infty} \frac{\varepsilon_{\text{old}}(l+1)(2l+1)l\theta^l}{\varepsilon_{\text{new}} l + \varepsilon_{\text{old}}(l+1)} \right] \times \\ & \times \left[8\sqrt{\theta} y_{\text{in1}}^3(\theta) - 6\sqrt{\theta} y_{\text{in1}}^2(\theta) \right]^{-1}, \\ \left(\frac{dz}{d\theta}\right)_{\text{out}}^{\text{max}} &= \\ &= \left[4y_{\text{out1}}^4(\theta) - 3y_{\text{out1}}^3(\theta) + p \sum_{l=0}^{\infty} \frac{\varepsilon_{\text{new}}(l+1)(2l+1)l\theta^{-(l+1)}}{\varepsilon_{\text{new}} l + \varepsilon_{\text{old}}(l+1)} \right] \times \\ & \times \left[8\sqrt{\theta} y_{\text{out1}}^3(\theta) - 6\sqrt{\theta} y_{\text{out1}}^2(\theta) \right]^{-1}. \end{aligned}$$

The values of z_{inter1} , z_{inter2} , θ_{inter1} and θ_{inter2} are found by solving the transcendent equation systems

$$\begin{cases} y_{\text{in1}}(\theta_{\text{inter1}}) = z_{\text{inter1}} + u, \\ y_{\text{in1}}(\theta_{\text{inter1}}) \sqrt{\theta_{\text{inter1}}} = z_{\text{inter1}}, \\ y_{\text{out1}}(\theta_{\text{inter2}}) = z_{\text{inter2}} - u, \\ y_{\text{out1}}(\theta_{\text{inter2}}) \sqrt{\theta_{\text{inter2}}} = z_{\text{inter2}}, \end{cases}$$

while θ_{max} is found from the solution to

$$y_{\text{out1}}(\theta_{\text{max}}) \sqrt{\theta_{\text{max}}} = z_{\text{max}}.$$

Equation (21) can be written as

$$\frac{J}{J_0} = 1 + nR_0^3 \exp\left[\frac{E_s}{3kT}\right] I, \quad (22)$$

where

$$I = I_{\text{in}} + I_{\text{inter}} + I_{\text{out}} - I_{\text{add}}. \quad (23)$$

In (23),

$$\begin{aligned} I_{\text{in}} &= \int_0^{\theta_{\text{inter1}}} 4\pi \sqrt{|f_{\text{in}}''(\theta)|} \exp\left[-\frac{E_s f_{\text{in}}^{\text{max}}(\theta)}{kT}\right] \times \\ & \times y_{\text{in1}}^2(\theta) \theta \left(\frac{dz}{d\theta}\right)_{\text{in}}^{\text{max}} d\theta; \quad (24) \end{aligned}$$

$$I_{\text{inter}} = \int_{z_{\text{inter1}}}^{z_{\text{inter2}}} 4\pi \sqrt{|f_{\text{inter}}''(z)|} \exp\left[-\frac{E_s f_{\text{inter}}^{\text{max}}(z)}{kT}\right] z^2 dz; \quad (25)$$

$$\begin{aligned} I_{\text{out}} &= \int_{\theta_{\text{inter2}}}^{\theta_{\text{max}}} 4\pi \sqrt{|f_{\text{out}}''(\theta)|} \exp\left[-\frac{E_s f_{\text{out}}^{\text{max1}}(\theta)}{kT}\right] \times \\ & \times y_{\text{out1}}^2(\theta) \theta \left(\frac{dz}{d\theta}\right)_{\text{out}}^{\text{max}} d\theta; \quad (26) \end{aligned}$$

$$I_{\text{add}} = \frac{4\pi z_{\text{max}}^3}{3} \exp\left[-\frac{E_s}{3kT}\right]. \quad (27)$$

Integrals (24)–(26) can be calculated only numerically. The values I_{in} , I_{out} and I_{inter} are proportional, respectively, to the contributions of ions inside and

outside the nuclei, and at the new-old phase interface to the nucleation rate J . Therefore, (22) is much more informative than (19) containing a double integral, which validates the use of the steepest descent method.

THEORY AND EXPERIMENT, COMPARED

The suggested theoretical model was applied to the case of vapor-liquid phase transition, when

$$N_1 = \frac{P}{kT}, \quad R_0 = \frac{2\sigma v}{kT \ln S}, \quad j = \frac{\alpha P}{\sqrt{2\pi m k T}}, \quad S = \frac{P}{P_{\text{eq}}},$$

(if the thermal equation of state for ideal gas is valid) [Strickland-Constable, 1968], where α is the condensation coefficient close to unity; m is the

molecular mass of the material subject to the phase transition; S is the vapor supersaturation; P is the vapor pressure; P_{eq} is the vapor-liquid equilibrium pressure. By varying the parameter q_0 included implicitly into (21), one can find such values $q = E_s q_0$ for some materials at which the theoretical results fit well the experimental data on critical vapor supersaturation S_{cr} at $n = 5.5 \cdot 10^5 \text{ cm}^{-3}$. The critical supersaturation S_{cr} corresponds to the case when $J = 1 \text{ cm}^{-3}/\text{s}$.

The theoretical results for a fixed q value are compared in Fig. 3 with experimental data reported by Rabeony and Mirabel [1987]. Additionally, the figure shows a curve of spontaneous nucleation calculated using (17), as well as a curve of ion-induced nucleation calculated on the basis of Thomson's mod-

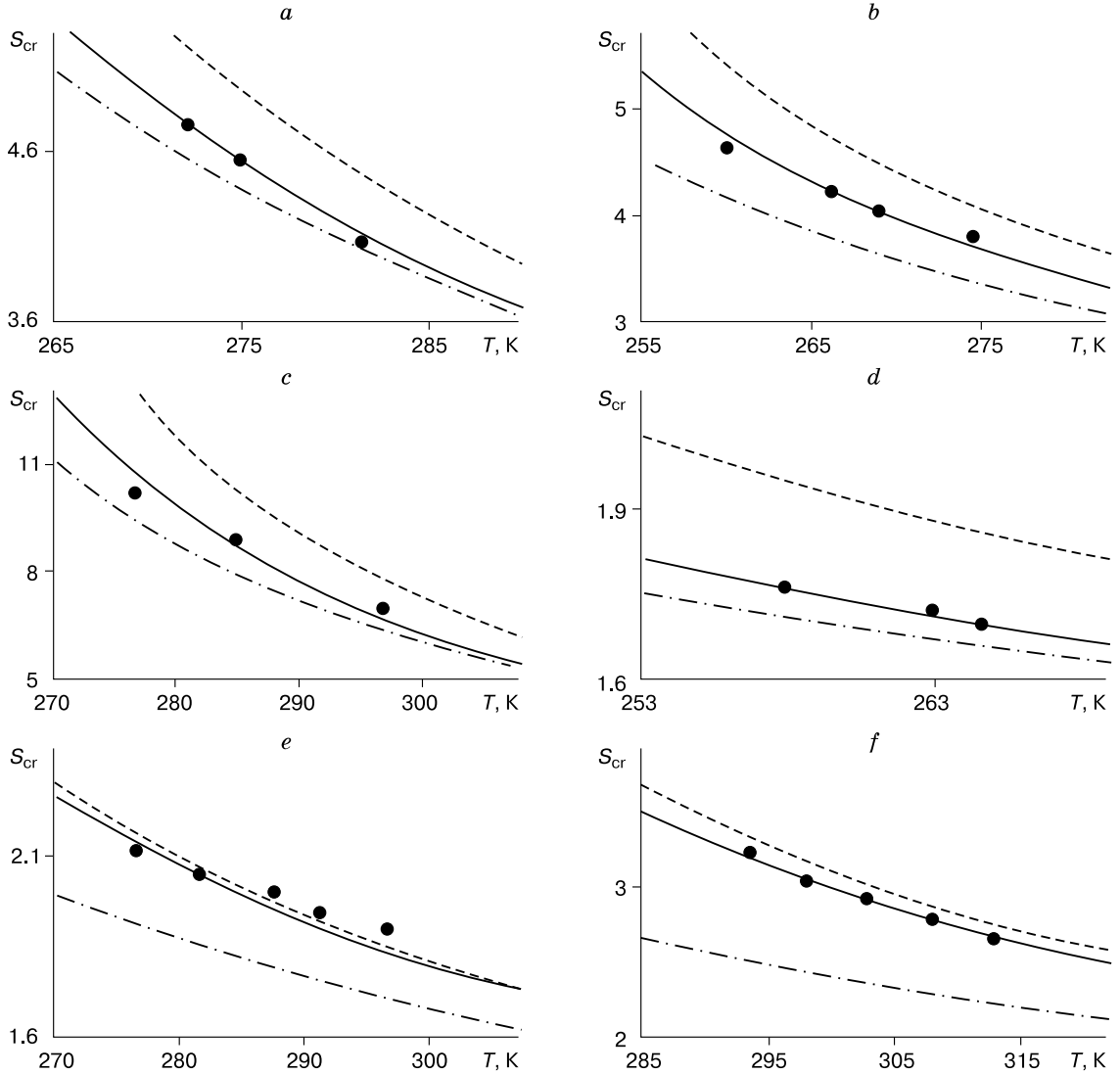


Fig. 3. Temperature dependence of critical vapor supersaturation for tetrachloromethane (a), trichloromethane (b), o-dimethylbenzene (c), methanol (d), ethanol (e), and water (f), at $n = 5.5 \cdot 10^5 \text{ cm}^{-3}$.

Points are experimental data [Rabeony and Mirabel, 1987]; solid line is theoretical curve at different q values: -1.30 eV (a), -1.45 eV (b), -1.43 eV (c), -1.70 eV (d), -1.34 eV (e), -1.84 eV (f); chain line is the curve of ion-induced nucleation according to Thomson's model; dash line is the curve of homogeneous nucleation ($n = 0$).

Table 1. Values of q corresponding to best fit between theory and experiment [Rabeony and Mirabel, 1987]

Tetrachloro- methane		Trichloro- methane		o-dimethyl- benzene		Methanol	
T, K	q, eV	T, K	q, eV	T, K	q, eV	T, K	q, eV
272.1	-1.29	260.0	-1.51	276.9	-1.49	258.0	-1.71
274.9	-1.30	266.2	-1.46	284.9	-1.42	263.0	-1.69
281.4	-1.32	268.8	-1.44	296.7	-1.39	264.6	-1.70
-	-	274.4	-1.39	-	-	-	-

el [Volmer, 1939; Kashchiev, 2000] assuming that each ion forms a stable associate and is a center of nucleation. The theoretical curves in Fig. 3 were obtained at $q = \text{const}$, but the best fit to the experiment was achieved by varying this parameter. The values of q corresponding to the best fit between the theory and the experiment for different materials obviously depend on temperature (Table 1, Fig. 3).

Note that most of the calculations were performed at $u = 0.4$. This dimensionless radius (in R_0 units) corresponds to the characteristic radius of the associate ion, i.e., an ion surrounded by molecules. The existence of such stable associates is consistent with the curve of local minimums in Fig. 2. Modeling shows that the magnitude of u causes only a minor effect on the final result. For example, the change in q was within 0.01 eV as u increased from 0.3 to 0.5.

CONCLUSIONS

The theory of single-component nucleation on ions has been presented above in its universal form applicable to any first-kind phase transition. It differs from the other existing theories of ion-induced nucleation as it implies the location of ions either inside or outside the cluster of the forming phase. Furthermore, it accounts for the energy of local interaction between the ion and the surrounding molecules in the explicit form (via q). Estimating the energy of this interaction is a separate research objective, but it can be found theoretically by matching calculations and experimental results.

The consideration above has focused on the case of nucleation when the static dielectric permittivity of the forming phase is larger than that of the old phase around the clusters. Meanwhile, similar modeling (using the steepest descent method) can be performed for the case when the new phase has a smaller static permittivity than the old phase.

References

- Anikin, G.V., 2004. The germ formation on nonzero volume ions. *Kriosfera Zemli VIII* (4), 54–55.
- Anikin, G.V., Plotnikov, S.N., 2005. The electric fields of ions: effect on nucleation work at first-kind phase transitions. *Zhurn. Fiz. Khimii* 79 (2), 363–367.
- Anikin, G.V., Plotnikov, S.N., 2007. The kinetic equation for heterogeneous nucleation near ions. *Kriosfera Zemli XI* (3), 63–70.
- Anisimov, M.P., 2003. Nucleation: theory and experiment. *Uspekhi Khimii* 72 (7), 664–705.
- Brodskaya, E., Lyubartsev, A.P., Laaksonen, A., 2002. Investigation of water clusters containing OH^- and H_3O^+ ions in atmospheric conditions. A molecular dynamics simulation study. *J. Chem. Phys.* 106 (25), 6479–6487.
- Dang, L.X., Smith, D.E., 1993. Molecular dynamics simulations of aqueous ionic clusters using polarizable water. *J. Chem. Phys.* 99 (9), 6950–6956.
- Fisenko, S.P., Kane, D.B., El-Shall, M.S., 2005. Kinetics of ion-induced nucleation in a vapor-gas mixture. *J. Chem. Phys.* 123 (10), article 104704 (10 p.).
- Hobbs, P.V., 1974. *Ice Physics*. Oxford Univ. Press, Oxford, 837 pp.
- Kashchiev, D., 2000. *Nucleation: Basic Theory with Applications*. Butterworth-Heinemann, Oxford, 530 pp.
- Kortzeborn, R.N., Abraham, F.F., 1973. Multistate kinetics in non-steady-state nucleation of water on gaseous ions. *J. Chem. Phys.* 58 (4), 1529–1534.
- Kusaka, I., Wang, Z.-G., Seinfeld, J.H., 1995a. Ion-induced nucleation: A density functional approach. *J. Chem. Phys.* 102 (2), 913–924.
- Kusaka, I., Wang, Z.-G., Seinfeld, J.H., 1995b. Ion-induced nucleation. II. Polarizable multipolar molecules. *J. Chem. Phys.* 103 (2), 8993–9009.
- Matveev, L.T., 1965. *Fundamentals of General Meteorology. Physics of the Atmosphere*. Gidrometeoizdat, Leningrad, 876 pp. (in Russian)
- Nadykto, A.B., Yu, F., 2004. Dipole moment of condensing monomers: A new parameter controlling the ion-induced nucleation. *Phys. Rev. Lett.* 93 (1), article 016101 (4 p.).
- Nadykto, A.B., Al Natsheh, A., Yu, F., et al., 2006. Quantum nature of the sign preference in ion-induced nucleation. *Phys. Rev. Lett.* 96 (12), article 125701 (4 p.).
- Rabeony, H., Mirabel, P., 1987. Experimental study of vapor nucleation on ions. *J. Chem. Phys.* 91 (7), 1815–1818.
- Rusanov, A.I., 1979. Thermodynamic theory of nucleation on charged particles. *J. Colloid Interface Sci.* 68 (1), 32–47.
- Rusanov, A.I., Kuni, F.M., 1984. Reformulation of the thermodynamic theory of nucleation on charged particles. *J. Colloid Interface Sci.* 100 (1), 264–277.
- Russell, K.C., 1969. Nucleation on gaseous ions. *J. Chem. Phys.* 50 (4), 1809–1816.
- Shevkunov, S.V., 2002a. Simulation of water clustering on chlorine ions. 1. Thermodynamic properties. *Kolloid. Zhurn.* 64 (2), 262–269.
- Shevkunov, S.V., 2002b. Simulation of water clustering on chlorine ions. 2. Microstructure. *Kolloid. Zhurn.* 64 (2), 270–279.
- Strickland-Constable, R.F., 1968. *Kinetics and Mechanism of Crystallization*. Elsevier Science & Technology Books, 347 pp.
- Thomson, J.J., Thomson, G.P., 1933. *Conduction of Electricity through Gases*. 3rd edition. Cambridge Univ. Press, Cambridge, 608 pp.
- Tohmfor, G., Volmer, M., 1938. Die Keimbildung unter dem Einfluss elektrischer Ladungen. *Ann. Phys.* 425 (2), 109–131.
- Toshev, B.V., 2002. Condensation on ions. *Electron. J. Math. Phys. Sci.* 1 (1), 120–126.
- Volmer, M., 1939. *Kinetik der Phasenbildung (Die Chemische Reaktion)*. Steinkopff, Dresden, 200 pp.
- Vorobiev, V.S., Malysenko, S.P., 2001. Phase formation by nucleation in electric fields. *ZHETF* 120 (4), 863–870.

Received June 1, 2012